

## **2<sup>1/2</sup> – DIMENSIONAL MOLD FILLING SIMULATIONS WITH A NON-NEWTONIAN AND NON-ISOTHERMAL FLUID USING UNSTRUCTURED MESHES**

### **Estacio, K. C.**

Departamento de Ciências de Computação e Estatística, Instituto de Ciências Matemáticas e de Computação, ICMC/USP, Av. Trabalhador São-Carlense, 400, C.P. 668, 13251-900, São Carlos, SP, Brasil  
kemelli@lcad.icmc.usp.br

### **Mangiavacchi, N.**

Departamento de Engenharia Mecânica, Universidade do Estado do Rio de Janeiro, UERJ, Rua São Francisco Xavier, 524, 20550-900, Rio de Janeiro, RJ, Brasil  
norberto@uerj.br

### **Tomé, M. F.**

murilo@lcad.icmc.usp.br

### **Cuminato, J. A.**

jacumina@lcad.icmc.usp.br

### **Castelo, A.**

castelo@lcad.icmc.usp.br

### **Nonato, L. G.**

gnonato@lcad.icmc.usp.br

Departamento de Ciências de Computação e Estatística, Instituto de Ciências Matemáticas e de Computação, ICMC/USP, Av. Trabalhador São-Carlense, 400, C.P. 668, 13251-900, São Carlos, SP, Brasil

***Abstract.** In this work a technique for the simulation of the filling stage of the injection molding process with a finite volume method and unstructured meshes is presented. The modified-Cross model with Arrhenius temperature dependence is employed to describe the viscosity of the melt. The temperature field is 3D and it is solved using a semi-Lagrangian scheme based on the finite volume method. The employed unstructured meshes are generated by Delaunay triangulation and the implemented numerical method uses the topological data structure SHE – Singular Handle Edge.*

***keywords:** Injection molding, non-Newtonian fluids, unstructured meshes, finite volume method, semi-Lagrangian formulation*

## **1. Introduction**

Fluid flows are governed by equations known as conservation equations: momentum conservation equation, mass conservation equation, also known as continuity equation, and energy conservation equation (Anderson Jr., 1995; Pantou, 1996).

Due to the governing equations complexity, obtaining analytical solutions is not trivial, and in many situations and applications, the numerical simulation requires the use of high efficiency numerical techniques and high performance computational resources. One of those applications is found in industries of manufacturing plastic products from injection of molten polymers, in a process called Injection Molding.

The flow of a fluid characterized by high viscosity in a narrow gap is a problem typically found in processes of injection molding. In this case, the flow can be described by few suitable simplifications in the three dimensional conservation equations, resulting in a formulation known as Hele-Shaw approach. This approach is also called 2<sup>1/2</sup>D approach, referring to limitations of the mould geometry to narrow, weakly curved channels. Thus the ratio of the cavity thickness and the characteristic length in the cavity mid-plane must be much less than unity.

In this work a technique for the simulation of the injection molding process of polymer is presented. This technique considers important aspects to guarantee the quality of the part, such as heat transfer by the walls and the points of insertion of the mold, and the influence of the temperature on the polymer fluidity. The implemented numerical method uses the topological data structure SHE – Singular Handle Edge (Nonato et al., 2002), which is capable to deal with boundary conditions and singularities, aspects commonly found in numerical simulations of fluid flow.

The governing equations are resolved using an unstructured mesh, generated by Delaunay triangulation (Shewchuk, 1999; Niceno, 2001) and the discretization method is based on the finite volume formulation (Baliga and Patankar, 1981; Maliska, 1995), using control volumes generated by the median method (Maliska, 1995).

## 2. The Governing Equations

The three-dimensional conservation equations, governing of the fluid motion, can be written as follow:

Continuity Equation

$$\frac{\partial \rho}{\partial t} + (\nabla \cdot \rho \vec{v}) = 0 \quad (1)$$

Momentum Equation

$$\frac{\partial}{\partial t}(\rho \vec{v}) = \rho \vec{g} + [\nabla \cdot \underline{\sigma}] - [\nabla \cdot \rho \vec{v} \vec{v}] \quad (2)$$

Energy equation

$$\rho c_p \left( \frac{\partial T}{\partial t} + \vec{v} \cdot \nabla T \right) = \beta T \left( \frac{\partial p}{\partial t} + \vec{v} \cdot \nabla p \right) + p \nabla \cdot \vec{v} + (\underline{\sigma} : \{\nabla \vec{v}\}) + \nabla \cdot (k \nabla T) \quad (3)$$

These equations are quite general and hold for all common fluids. With current computers, solving them in complicated domains, as required to simulate injection molding with cavities, is still a very difficult task. In the last two decades, several researchers have been trying to analyze the injection molding process using different simplifications and approaches limited by the available computational resources (Vasconcellos, 1999; Chang and Yang, 2001). Thus, to obtain solutions in real time some suppositions using data for most commonly employed materials are employed with the aim of promoting simplifications in the governing equations.

Such simplifications can be done on Eq. (1), (2) and (3), using the following assumptions:

- i. During the filling phase, the fluid is considered incompressible;
- ii. The fluid is considered a Generalized Newtonian Fluid;
- iii. The thermal conductivity of the material is assumed constant;
- iv. Dimensional analysis is employed to eliminate low magnitude terms in each equation;

Using the above assumptions about material behavior and dimensional analysis, equations (1) to (3) are reduced to the following:

Continuity Equation

$$\frac{\partial v_x}{\partial x} + \frac{\partial v_y}{\partial y} + \frac{\partial v_z}{\partial z} = 0 \quad (4)$$

Momentum Equations

$$\frac{\partial p}{\partial x} = \frac{\partial}{\partial z} \left( \eta \frac{\partial v_x}{\partial z} \right), \quad \frac{\partial p}{\partial y} = \frac{\partial}{\partial z} \left( \eta \frac{\partial v_y}{\partial z} \right), \quad \frac{\partial p}{\partial z} = 0 \quad (5)$$

Energy Equation

$$\rho c_p \left( \frac{\partial T}{\partial t} + v_x \frac{\partial T}{\partial x} + v_y \frac{\partial T}{\partial y} \right) = \eta \dot{\gamma}^2 + k \frac{\partial^2 T}{\partial z^2} \quad (6)$$

Further simplification is possible by integrating the momentum and continuity equations, realizing that the pressure field is two-dimensional, as shown by Eq. (5).

- v. Simplification by mathematical analysis.

In order to obtain an expression for the pressure, which is a function of  $x$  and  $y$  only, it is convenient to integrate the momentum and continuity equations across the thickness. The resulting equation is called Hele-Shaw equation:

$$\frac{\partial}{\partial x} \left( S_2 \frac{\partial p}{\partial x} \right) + \frac{\partial}{\partial y} \left( S_2 \frac{\partial p}{\partial y} \right) = 0 \quad (7)$$

where  $S_2$  is called fluidity.

For symmetrical molds  $S_2$  is defined by:

$$S_2 = \int_0^h \frac{z'^2}{\eta} dz' \quad (8)$$

### 3. Resulting Equations

After those assumptions, the governing equations for the average quantities of the fluid flow, during mold filling, can be written as:

$$\frac{\partial}{\partial x} \left( S_2 \frac{\partial p}{\partial x} \right) + \frac{\partial}{\partial y} \left( S_2 \frac{\partial p}{\partial y} \right) = 0 \quad (9)$$

$$\rho c_p \left( \frac{\partial T}{\partial t} + v_x \frac{\partial T}{\partial x} + v_y \frac{\partial T}{\partial y} \right) = \eta \dot{\gamma}^2 + k \frac{\partial^2 T}{\partial z^2} \quad (10)$$

In this work the fluid flow field is considered symmetric, therefore the equations for components  $v_x$  and  $v_y$  of the velocity must be computed only for half of mold and are given for:

$$v_x = -\frac{\partial p}{\partial x} \left( \int_0^z \frac{z'}{\eta} dz' - \int_0^h \frac{z'}{\eta} dz' \right) \quad \text{and} \quad v_y = -\frac{\partial p}{\partial y} \left( \int_0^z \frac{z'}{\eta} dz' - \int_0^h \frac{z'}{\eta} dz' \right) \quad (11)$$

The equations (9) and (10) are solved using the finite volume method on an unstructured mesh, generated by the EasyMesh, a two-dimensional mesh generator based on Delaunay triangulation (Niceno, 2001). All the calculations are elaborated using the topological data structure SHE – *Singular Handle Edge* (Nonato et al., 2002).

#### 3.1. Boundary Conditions

For the injection molding problem, boundary conditions connect the solution of the pressure and thermal distributions in the cavity. Actually, the equation of the pressure (9) is coupled to the equation of the energy (10) since the viscosity of the material, which affects the pressure, is determined by both temperature and shear rate.

The equations (9) and (10) should be solved subject to the following boundary conditions:

1. Assuming the molds are vented, the pressure is zero at the free surface;
2. The pressure or the flow rate is defined in the inlet regions;
3. The pressure gradient in the normal direction is zero in any impermeable boundary;
4. The temperature in the cavity wall or in some interior point to the wall is defined;
5. The temperature gradient in the  $z$ -direction is zero in the center plane of the cavity;
6. The melt temperature is defined in the inlet regions.

#### 3.2. Viscosity Model

The viscosity model chosen in this work is the modified-Cross Model with Arrhenius temperature dependence (Chang and Yang, 2001):

$$\eta(T, \dot{\gamma}) = \frac{\eta_0(T)}{1 + \left( \eta_0 \frac{\dot{\gamma}}{\tau^*} \right)^{1-n}} \quad \text{with} \quad \eta_0(T) = B \exp \left( \frac{T_b}{T} \right) \quad (12)$$

where  $n$  is the power law index,  $\eta_0$  is the zero shear viscosity,  $\tau^*$  is the parameter that describes the transition region between zero shear rate and the power law region of the viscosity curve. For polystyrene, the model constants are given by  $n = 0,2838$ ,  $B = 2,591 \times 10^{-7} Pa \cdot s$  and  $\tau^* = 1,791 \times 10^4 Pa$ ,  $T_b = 11680 K$ . The density, the specific heat and the thermal conductivity are, respectively, given for  $\rho = 940 Kg/m^3$ ,  $c_p = 2100 J/Kg K$  and  $k = 0,18 W/m K$  (Chen et al., 1998).

### 4. The Solution Process

The numerical solution of the governing equation for the filling phase is done in three main stages: calculation of the pressure field, calculation of the temperature field and, finally, advancement of the free surface (Kennedy, 1995).

Since the fluidity depends on the viscosity, which in turn depends on both temperature and shear rate, the equations (9) and (10) must be solved simultaneously. However, for the numerical solution, the equations can be decoupled using small time increments (steps). At a particular time, the temperature is assumed constant and the pressure field is calculated assuming a value for the viscosity at that temperature. Making sure that the time steps are sufficiently small, this procedure guarantees satisfactory results.

The sequence of the solution process is as follows:

1. Solution of pressure equation

- (a) Calculation of  $S_2$ ;
- (b) Calculation of the pressure field;
- (c) Determination of the velocity field;
- (d) Determination of the shear rate;
- (e) Calculation of the viscosity;

The steps of (a) to (e) are repeated until the variation of the pressure, in two successive iterations, is smaller than a defined tolerance.

2. Solution of the temperature equation

- (a) Calculation of the convective and the viscous heating terms;
- (b) Calculation of conduction term;

3. Moving the free surface

- (a) Since the flow rate is known in each control volume, it is possible to choose the time increment such that only one control volume will fill in the next time-step. Therefore, the free surface is advanced appropriately.

The pressure equation is solved using a Finite Volume Method. The prediction of the free surface position is obtained by a Volume Tracking Method, and the temperature equation is solved using a Finite Volume Method for the calculation of the convective and viscous heating terms and a Finite Difference Method for the calculation of the conduction term and for the time progress.

**5. Solution of Pressure Equation**

Defining the flux  $\vec{J}$  by  $\vec{J} = -S_2 \nabla p$ , the pressure equation (9) can be written as:

$$\nabla \cdot \vec{J} = 0 \tag{13}$$

Similarly to other methods for obtaining approximated equations from balance equations, the procedure of the finite volume method consists on the integration of the differential equation in the conservative form in the control volume. An example of control volume created by the median method and utilized in this work is shown in the Fig. 1, where it can be seen that it is composed by contributions of several elements of the type  $\overline{123}$ .

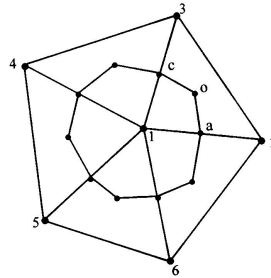


Figure 1: Control volume for the median method (Maliska, 1995).

Integrating Eq. (13) in the control volume and applying the Gauss Divergence Theorem, it results:

$$\int_S \vec{J} \cdot \vec{n} dS = 0 \tag{14}$$

where  $S$  is the closed boundary of  $V$  and  $\vec{n}$  is an unit outward normal to  $S$ .

The surface integral, calculated in the control volume of the vertex 1, as illustrated in the Fig. 1, results in:

$$\int_a^0 \vec{J} \cdot \vec{n} dS + \int_0^c \vec{J} \cdot \vec{n} dS + [contributions from other elements associated to node 1] = 0 \tag{15}$$

Since the flux  $\vec{J}$  depends on the partial derivatives of  $p$ , the integration given by the equation (15) requires the value of those derivatives along the lines  $\overline{a0}$  and  $\overline{0c}$ . However, the values of  $p$ , are stored in the vertices of the triangular elements. It is necessary, therefore, to establish an interpolation function for  $p$ . The chosen interpolation function for  $p$  is:

$$p = Ax + By + C \tag{16}$$

With the values of  $p_1$ ,  $p_2$  and  $p_3$  and the values of the coordinates  $(x, y)$  in the points 1, 2 and 3, it is possible to find out the values of constant  $A$ ,  $B$  and  $C$ , which are given by:

$$A = \frac{[(y_2 - y_3)p_1 + (y_3 - y_1)p_2 + (y_1 - y_2)p_3]}{D} \quad (17)$$

$$B = \frac{[(x_3 - x_2)p_1 + (x_1 - x_3)p_2 + (x_2 - x_1)p_3]}{D} \quad (18)$$

$$C = \frac{[(x_2y_3 - x_3y_2)p_1 + (x_3y_1 - x_1y_3)p_2 + (x_1y_2 - x_2y_1)p_3]}{D} \quad (19)$$

where:

$$D = (x_1y_2 + x_2y_3 + x_3y_1 - y_1x_2 - y_2x_3 - y_3x_1) \quad (20)$$

Recalling that the flux vector is given by:

$$\vec{J} = (J_x, J_y) = \left( -S_2 \frac{\partial p}{\partial x}, -S_2 \frac{\partial p}{\partial y} \right) \quad (21)$$

and that it is possible to obtain the partial derivatives of  $p$  with respect to  $x$  and  $y$  using the interpolation function (16), the component  $J_x$  and  $J_y$  result in:

$$J_x = -AS_2, \quad J_y = -BS_2 \quad (22)$$

Substituting the expressions of Eq. (22) in Eq. (15), it is possible to calculate the integrals along  $\overline{a0}$  and  $\overline{0c}$ :

$$\int_S \vec{J} \cdot \vec{n} dS = \int_a^0 \vec{J} \cdot \vec{n} dS + \int_0^c \vec{J} \cdot \vec{n} dS = AS_2(y_a - y_c) + (BS_2)(x_c - x_a) \quad (23)$$

Substituting the expressions for  $A$  and  $B$  in Eq. (23), the integration along the surface  $S$  of the element  $\overline{123}$  relative to the control volume associated to the vertex 1 results in:

$$\int_a^0 \vec{J} \cdot \vec{n} dS + \int_0^c \vec{J} \cdot \vec{n} dS = C_{11}p_1 + C_{12}p_2 + C_{13}p_3 \quad (24)$$

where the coefficients are given by:

$$C_{11} = \frac{S_2}{D} [(y_a - y_c)(y_2 - y_3) + (x_a - x_c)(x_2 - x_3)] \quad (25)$$

$$C_{12} = \frac{S_2}{D} [(y_a - y_c)(y_3 - y_1) + (x_a - x_c)(x_3 - x_1)] \quad (26)$$

$$C_{13} = \frac{S_2}{D} [(y_a - y_c)(y_1 - y_2) + (x_a - x_c)(x_1 - x_2)] \quad (27)$$

The contribution for the control volumes of the vertices 2 and 3 can be computed analogously. Calling

$$p_e = [p_1 \quad p_2 \quad p_3]^t \quad (28)$$

the vector of the pressures in the element  $\overline{123}$ , the contribution for the control volumes of the element  $\overline{123}$ , associated to the vertices 1, 2 and 3 of the element  $e$ ,

$$u_e = [u_1 \quad u_2 \quad u_3]^t \quad (29)$$

can be calculated by  $u_e = C_e p_e$  where  $C_e$  is a  $3 \times 3$  matrix constituted by the coefficients  $C_{ij}$ , with  $1 \leq i, j \leq 3$  of the vertices 1, 2 and 3.

The calculation of matrix  $C_e$ , and consequently, of the contribution  $u_e$ , is made for each mesh element. Therefore, it is necessary to add all the contributions due to all the  $n$  mesh elements. As the elements and the vertices of the mesh are enumerated, a procedure to add these contributions consists of calculating the matrix  $C_e$  of the elements and to assemble a sparse matrix  $K$ , of dimension  $n \times n$ . The contributions for the vector  $u_e$ , in the case of prescribed pressure, are mounted in vector  $F$ , resulting in the linear system:

$$K p = F \quad (30)$$

This linear system is symmetric and it is solved by the Conjugate Gradient Method. After obtaining the solution, the values of  $p$  are determined in all the vertices of the triangular grid, that is, at the center of the control volumes where the conservation balance of the pressure  $p$  were computed.

There are two convergence criteria applied on pressure calculation. The first one is employed in the Conjugate Gradient Method inner iteration, and it was established as  $\varepsilon_1 = 10^{-7}$ . The second one is employed in the outer iteration, described on Section 4, item 1, where the  $l_2$  norm of the difference between the pressure at two consecutive iterations must be lower than  $\varepsilon_2 = 10^{-7}$ .

## 6. Moving the Free Surface

For the identification and the advancement of the fluid free surface, the Volume of Fluid (VOF) technique (Ransau, 2002) is used. This strategy consists in the application of the mass conservation equation, in the integral form,

$$\int_V \left( \frac{\partial \phi}{\partial t} + \nabla \cdot (\vec{v}\phi) \right) dV = 0 \quad (31)$$

where  $\phi$  is the filling factor, to the control volume which involves a vertex and in the discretization of the equation in the usual way employing finite volumes.

This filling factor ranges to 0 to 1: if  $\phi$  of a vertex is equal to 1, means that the associated control volume is completely full of fluid and if  $\phi$  of the vertex is equal to 0, then the associated control volume associated is completely empty. Intermediate values of  $\phi$  indicate that the control volume is partially full and represent the free surface position.

After calculation of the time derivative of the  $\phi$  factor,  $\left(\frac{\partial \phi}{\partial t}\right)$ , for all mesh vertices, it is possible to calculate the time step,  $dt$ , that is necessary to accurately fill one control volume associated with a vertex whose  $0 \leq \phi \leq 1$ . At each time step, the time interval is chosen such that only one control volume is filled. The flux on Eq. (31) are computed only for full control volumes. This strategy does not demand specific treatment for any control volumes and results in a scheme with low numerical diffusion.

## 7. Solution of Temperature Equation

The chosen strategy to calculate the contributions of the temperature field is a semi-Lagrangian method (Phillips and Williams, 2001). The basic idea is to follow a particle during its trajectory over the mesh.

Consider the energy equation (10) written in terms of the material derivative, as follow:

$$\frac{DT}{Dt} = f \quad \text{where} \quad f = \frac{1}{\rho c_p} \left( \eta \dot{\gamma}^2 + k \frac{\partial^2 T}{\partial z^2} \right) \quad (32)$$

which can be evaluated as

$$\frac{T(p_a, t + dt) - T(p_a, t)}{dt} = f \quad (33)$$

where  $p_a$  is an arbitrary particle. Choosing a particle that occupies the position of a vertex at time  $t + dt$  and writing this expression in terms of coordinates  $\vec{x} = (x, y)$ , we have:

$$T(\vec{x}, t + dt) = T(\vec{x} - d\vec{x}, t) + dt f \quad (34)$$

where  $d\vec{x} = \vec{v} dt$ . Notice that  $\vec{x}$  is the position occupied in the time  $t + dt$  by a fluid particle that occupied the position  $\vec{x} - d\vec{x}$  in the time  $t$ . Considering a linear approximation for  $T$  in the triangle that contains  $\vec{x}$ , then  $T(\vec{x} - d\vec{x}, t)$  can be approximated using a truncated Taylor expansion:

$$T(\vec{x} - d\vec{x}, t) = T(\vec{x}, t) - d\vec{x} \cdot \nabla T \quad (35)$$

Substituting the expression (35) in (34), it is obtained:

$$T(\vec{x}, t + dt) = T(\vec{x}, t) - dt \vec{v} \cdot \nabla T + dt f \quad (36)$$

where  $\nabla T$  is computed at the element that contains the particle  $p_a$  at time  $t$ , that is,  $\nabla T = \nabla T(\vec{x} - d\vec{x}, t)$ , and  $\vec{v}$  is the velocity at the vertex.

### 7.1. Calculating the Convection Term

The term of the temperature equation which represents the convection in the fluid flow is given by the product  $\vec{v} \cdot \nabla T$ . The calculation of the gradient of  $T$  is analogously made to the of the pressure gradient, using a linear interpolation. The choice of the value of the velocity and temperature gradient to compute the product  $\vec{v} \cdot \nabla T$ , for each vertex, is made as follow:

1. For each triangle
  - (a)  $\frac{\partial T}{\partial x}$  and  $\frac{\partial T}{\partial y}$  are calculated according to the interpolation function for  $T$ ;
2. For each triangle vertex, it is verified if a particle  $p_a$  at the vertex at the time  $t + dt$ , is originated from this triangle (element) at the time  $t$  performing the following steps:
  - (a) the vector product is calculated between the velocity vector in the cell and the vectors that compose the incident edges to that vertex;
  - (b) If those two products have different signs, then the particle  $p_a$  belongs to that triangle and therefore, the product  $\vec{v} \cdot \nabla T$  can be done with the value of the velocity at that vertex. The result is stored in the vertex corresponding to the coordinate  $\vec{x}$ .

## 7.2. Calculating the Viscous Heating Term

The term of the temperature equation that represents the viscous dissipation in the fluid flow is given by  $\eta\dot{\gamma}^2$ , with shear rate  $\dot{\gamma}$  given by  $\dot{\gamma} = \sqrt{\left(\frac{\partial v_x}{\partial z}\right)^2 + \left(\frac{\partial v_y}{\partial z}\right)^2}$ .

The derivatives  $\frac{\partial v_x}{\partial z}$  and  $\frac{\partial v_y}{\partial z}$  can be obtained using the equations of components  $v_x$  and  $v_y$  of the velocity that, for a symmetrical flow, are given by the equation (11). When those expressions are substituted in the expression of the shear rate, we have:

$$\dot{\gamma} = \frac{z}{\eta} |\nabla p| \quad (37)$$

Substituting the expression of the viscosity (12) in the equation (37), the shear rate can be written as:

$$\dot{\gamma} = |\nabla p| \frac{z}{\eta_0} \left[ 1 + \left( \eta_0 \frac{\dot{\gamma}}{\tau^*} \right)^{1-n} \right] \quad (38)$$

Defining a function  $G = G(\dot{\gamma})$  as:

$$G(\dot{\gamma}) = \dot{\gamma} - |\nabla p| \frac{z}{\eta_0} \left[ 1 + \left( \eta_0 \frac{\dot{\gamma}}{\tau^*} \right)^{1-n} \right] \quad (39)$$

it is possible to use Newton's method and to find the root of that equation, using the following iteration function:

$$\dot{\gamma}^{k+1} = \dot{\gamma}^k - \frac{G(\dot{\gamma}^k)}{G'(\dot{\gamma}^k)} \quad (40)$$

where  $G'(\dot{\gamma}^k)$  the derivative of  $G(\dot{\gamma}^k)$  with respect to the  $\dot{\gamma}^k$ .

By knowing, then, the value of the shear rate for a certain value of  $z$ , the value of the viscosity in this thickness is determined using the equation (12), and, finally, the product of that variable for the square of the shear will result in the value of the viscous dissipation in that point.

## 7.3. Calculating the Conduction Term

The conduction, represented by the term  $k \frac{\partial^2 T}{\partial z^2}$ , is approached by a centered finite difference scheme, respecting the boundary conditions for the temperature:

$$k \frac{\partial^2 T}{\partial z^2} = k \frac{T_{i,k+1} - 2T_{i,k} + T_{i,k-1}}{dz^2} \quad (41)$$

where the index  $i$  varies with the coordinates  $(x, y)$  of the mesh and the index  $k$ , with the coordinate  $z$ . The finite difference mesh in the space direction  $z$  is defined as a mesh of  $N_z$  layers and with a spacing  $dz = \frac{h}{N_z}$ .

## 7.4. Solution of Temperature Equation

After having established the strategies for the solution of the energy equation in the space directions  $x$ ,  $y$  and  $z$ , it is necessary to establish the strategies for the transient solution. The evaluation of the temperature at the time  $n + 1$ , is done in the following way: the convective and viscous heating terms are evaluated in the time  $n$ , and the conduction term will define the employed finite difference scheme, which could be evaluated in the time  $n$ , resulting in an explicit scheme, in the time  $n + 1$ , resulting in an implicit scheme, or in both times, by making an average between them, resulting in an Crank-Nicolson scheme.

## 8. Results

The solution of the pressure distribution has been validated considering constant fluidity against analytical solutions (the melt is considered as a Newtonian fluid and the fluid flow is considered isothermal). The energy equation solution has been validated against an one-dimensional analytical solution of the transport of a sharp temperature discontinuity by a constant velocity field (Estacio, 2004; Estacio and Mangiavacchi, 2004). In this section we present two representative results of solving equations (9) and (10) for general situations, using prescribed inlet velocity. The simulation data are: inlet temperature  $T = 513 K$ , the wall temperature  $T_w = 313 K$ , the prescribed velocity  $v_0 = 10^{-2} m/s$ , the reference

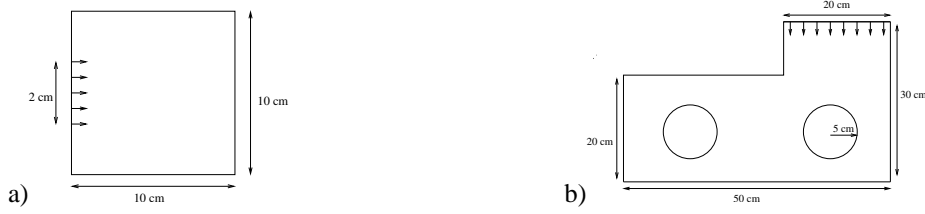


Figure 2: Molds used in the simulations: 2(a) rectangular mold and 2(b) complex l-shaped mold with two circular insertions.

inlet prescribed pressure  $p_0 = 10^5 \text{ N/m}^2$ , mold thickness  $h = 10^{-2} \text{ m}$  and number of layers for the solution of the three-dimensional energy equation  $N_z = 5$ . The material properties are the same as the ones described in Section 3.2.

The first simulation was conducted using a rectangular mold, whose dimensions are shown in Fig. 2(a). The unstructured triangular mesh built on the rectangular mold has 313 elements. This relatively coarse grid was chosen for this test because it produces better visualization of results. For the temperature field, only the elements completely full of fluid are shown with the purpose of illustrating the advancing of the free surface. The time steps employed in this simulation range from 0,0066 to 1,6466 seconds with an average value of 0,2795 seconds. The figures 3, 4 and 5 show the pressure, the velocity vector and the three-dimensional temperature fields at the center plane of the cavity, respectively. They show four stages of the mold filling, ordered as follow: right after the flow had started, at  $t = 5.09 \text{ s}$ ; at two intermediate times,  $t = 17.23 \text{ s}$  and  $t = 31.75 \text{ s}$ ; and near the end of the injection, when  $t = 46.37 \text{ s}$ .

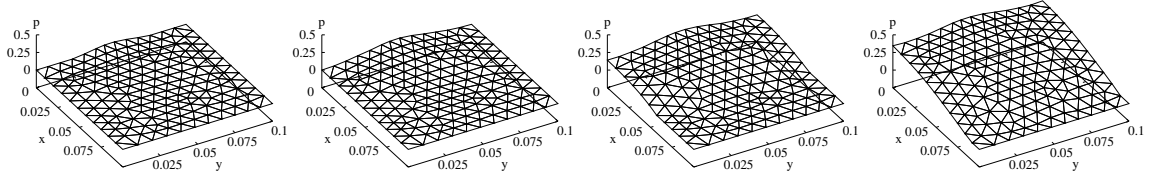


Figure 3: Four stages of pressure solution for a rectangular mold. The values are scaled by  $p_0$ .

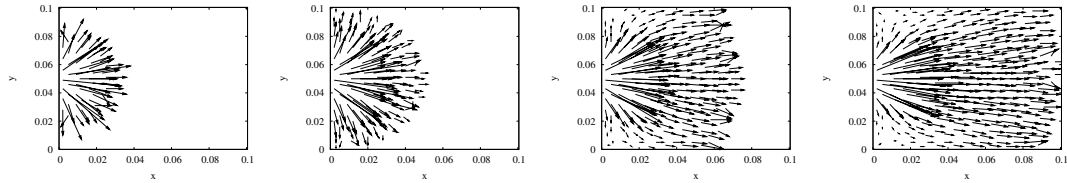


Figure 4: Velocity vectors obtained after the calculations for the pressure distribution.

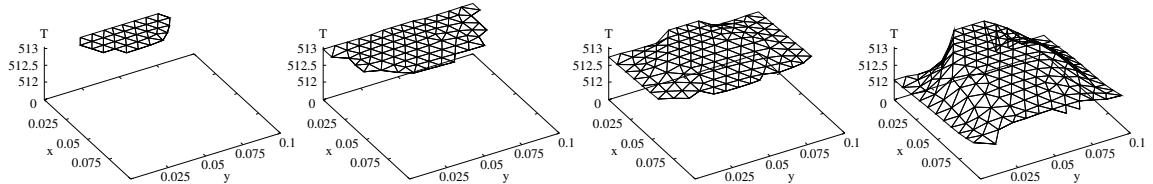


Figure 5: Four stages of the temperature distribution at the cavity center plane, i.e.,  $z = 0$ , during the mold filling with prescribed velocity.

According to mass conservation, the exact time for the mold filling is 50 seconds and, according to the simulation, the necessary time of injection for the total mold filling was 49.41 seconds, which corresponds to an 1.18 % error. Simulating the fluid flow in the conditions described previously, but using a mesh with 1003 elements, the predicted time of injection becomes  $t = 49.82 \text{ s}$ , resulting in an 0.36 % error.

The profiles of the temperature distribution along the mold, that is, the evolution of the temperature distribution with respect to both mold length and the layer, are presented in the Fig. 6. This simulation was done also considering 13 and 21 layers for the discretization in  $z$ -direction. Therefore, the approaches for the profiles of the three-dimensional temperature in the common layers of the mold can be compared. In this case, the common layers happen when  $z = 0$ ,  $z = 0,0025$ ,

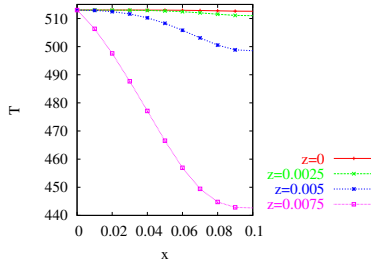


Figure 6: Profiles of the three-dimensional temperature distribution of along the mold, for the point  $(x, y)$  such that  $y = 0,05$  and  $0 \leq x \leq 0,1$  plotted for the layers  $z = 0, z = 0,0025, z = 0,005$  and  $z = 0,0075$  m, respectively, at the end of the injection. The temperature of the last layer ( $z = 0,01$ ) is prescribed and given by  $T_w = 313$  K.

$z = 0,005$  and  $z = 0,0075$  meters, and the comparison among them is illustrated in the Fig. 7. For a better visualization of the considered results, some layers of the discretization in the  $z$ -direction were omitted.

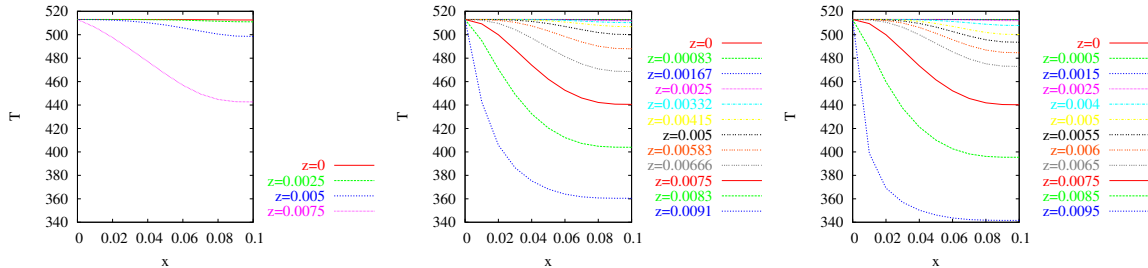


Figure 7: Profiles of the distribution of the three-dimensional temperature along the mold, for the point  $(x, y)$  such that  $y = 0,05$  and  $0 \leq x \leq 0,1$ , using 5, 13 and 21 layers, respectively. The temperature of the last layer ( $z = 0,01$ ) is prescribed and given by  $T_w = 313$  K.

A l-shaped mold with two circular insertions, whose dimensions are shown in Fig. 2(b) was used in the second simulation. The unstructured triangular mesh built on the mold has 563 elements and the time steps employed in this simulation range from 0,0008 to 1,4856 seconds with an average value of 0,1783 seconds.

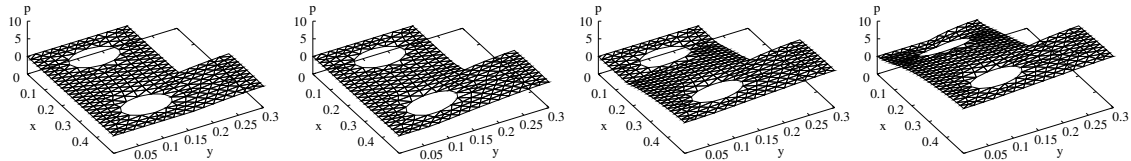


Figure 8: For stages of the pressure solution for a l-shaped mold with two circular insertions using prescribed velocity. The values are scaled by  $p_0$ .

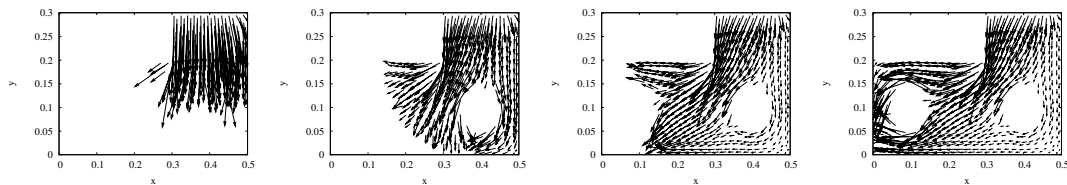


Figure 9: Velocity vectors obtained after the calculations for the pressure distribution.

The figures 8, 9 and 10 show the pressure, the velocity vector and the temperature fields at the center plane of the cavity, respectively, during the numerical simulation of the l-shaped mold filling. They show four stages of the filling of the mold: right after the flow had started, at  $t = 15.38$  s; at two intermediate times,  $t = 37.21$  s and  $t = 46.41$  s; and near the end of the injection, when  $t = 56.53$  s. In this second simulation, it is possible to observe the capability of the present model to deal with splitting and remerging of the free-surface/melt front during the filling process. The prediction and localization of this effect are essential to guarantee the final quality of the part since the remerging regions are one of the most fragile areas of the molded part.

The predicted injection time is 57.48 s, and the exact time, based on mass conservation is 52.5 s, resulting in an 8.41% error which is quite large. However, using a finer mesh with 5546 elements, the predicted injection time is given

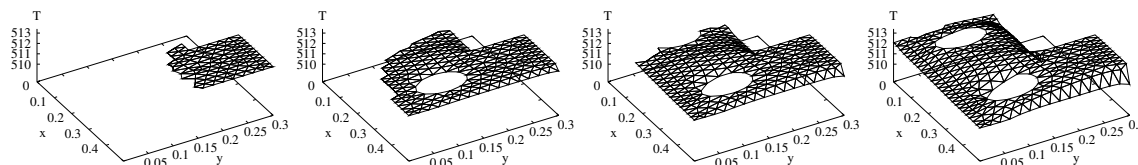


Figure 10: Four stages of the temperature distribution at the cavity center plane, i.e.,  $z = 0$ .

by 52.61 s, resulting in an 0.20% error.

## 9. Conclusion

This work presented a finite volume method over an unstructured mesh for solving the governing equations of fluid flow during the filling phase of injection molding. This methodology allows to simulate complex geometries without excessive computational efforts, producing temperature and shear stress distributions and real injection times. Thus, the proposed method may be considered an useful tool for the design, analysis and troubleshooting of injection molding process. This fast and simple prediction tool provides a 3-dimensional temperature distribution, including heat transfer and viscous dissipation effects, which is sufficiently accurate for most applications.

The meshes used in the simulations can be considered coarse, but the choice was based on a better visualization of the obtained data. However, using finer meshes in those problems, it is noticed a decrease in the numerical error in all the cases, what means that the implemented method is convergent.

## 10. Acknowledgments

We gratefully acknowledge support given by FAPESP (grant 01/10758-0) and CNPq (grant 302633/2003-0).

## 11. References

- Anderson Jr., J. D., 1995, “Computational Fluid Dynamics - The Basics with Applications”, McGraw-Hill, New York.
- Baliga, B. R. and Patankar, S. V., 1981, A New Finite Element Formulation for Convection-Diffusion Problems, “Numerical Heat Transfer”, Vol. 3, pp. 393–409.
- Chang, R.-Y. and Yang, W.-H., 2001, Numerical Simulation of Mold Filling in Injection Molding using a Three-Dimensional Finite Volume Approach, “Int. J. Numer. Meth. Fluids”, Vol. 37, pp. 125–148.
- Chen, S. C., Chen, Y. C., and Cheng, N. T., 1998, Simulation of Injection-Compression Mold-Filling Process, “Int. Comm. Heat Mass Transfer”, Vol. 25, No. 7, pp. 907–917.
- Estacio, K. C., 2004, Simulação do Processo de Moldagem por Injeção 2D usando Malhas Não Estruturadas, Master’s thesis, Universidade de São Paulo, São Carlos.
- Estacio, K. C. and Mangiavacchi, N., 2004, Two-Dimensional Mold Filling Simulation With a Non-Newtonian Fluid and Unstructured Meshes, “Proceedings of the CONEM-2004 - III National Congress of Mechanical Engineering”, Belém - PA. ABCM, CD-ROM.
- Kennedy, P., 1995, “Flow Analysis of Injection Molds”, Hanser Publishers, New York.
- Maliska, C. R., 1995, “Transferência de Calor e Mecânica dos Fluidos Computacional - Fundamentos e Coordenadas Generalizadas”, LTC - Livros Técnicos e Científicos, Rio de Janeiro.
- Niceno, B., 2001, Easymesh: a Free Two-Dimensional Quality Mesh Generator Based on Delaunay Triangulation, Available in <<http://www.dinma.univ.trieste.it/nirftc/research/easymesh/Default.htm>>, Accessed in: April 12th, 2004.
- Nonato, L. G., Castelo F<sup>o</sup>, A., and Oliveira, M. C. F., 2002, A Topological Approach for Handling Triangle Insertion and Removal into Two-Dimensional Unstructured Meshes, Available in <<http://citeseer.nj.nec.com/551625.html>>, Accessed in: April 12th, 2004.
- Panton, R. L., 1996, “Incompressible flow”, Wiley Interscience, New York, 2nd. edition.
- Phillips, T. N. and Williams, A. J., 2001, A Semi-Lagrangian Finite Volume Method for Newtonian Contraction Flows, “SIAM Journal on Scientific Computing”, Vol. 22, No. 6, pp. 2152–2177.
- Ransau, S. R., 2002, Solution Methods for Incompressible Viscous Free Surface Flows: A Literature Review, Available in <<http://www.math.ntnu.no/preprint/numerics/2002/>>, Accessed in: April 12th, 2004.
- Shewchuk, J. R., 1999, Lecture Notes on Delaunay Mesh Generation, Available in <<http://citeseer.nj.nec.com/shewchuk99lecture.html>>, Accessed in: April 12th, 2004.
- Vasconcellos, J. F. V., 1999, “Um método de Volumes Finitos Usando Malhas Não Estruturadas para o Estudo de Escoamentos com Frentes Livres”, PhD thesis, Universidade Federal de Santa Catarina, Florianópolis.